Cell Reports
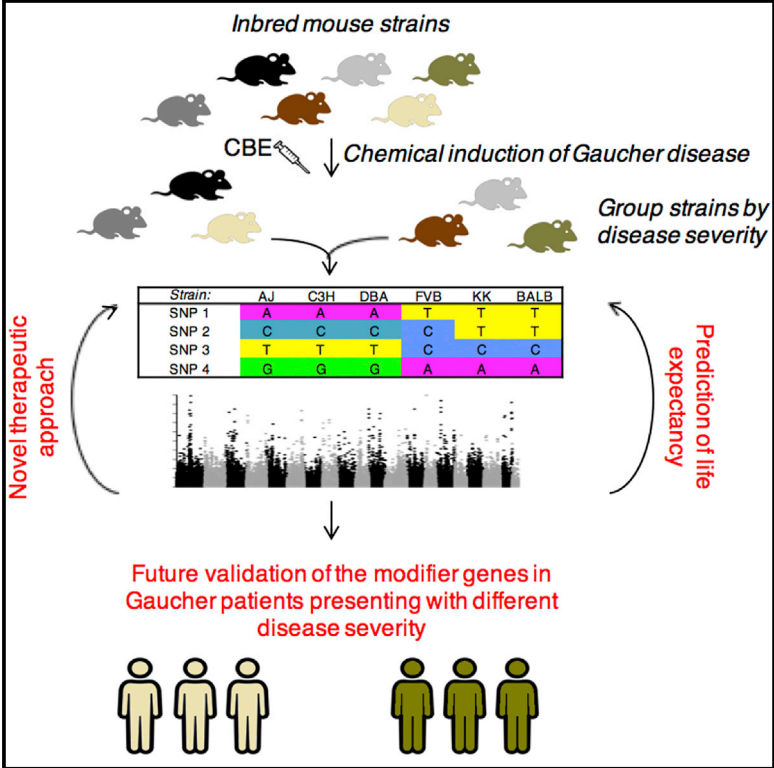
Identification of Modifier Genes in a Mouse Model of Gaucher Disease

Graphical Abstract

Authors

Andrés D. Klein, Natalia-Santos Ferreira, Shifra Ben-Dor, ..., Timothy M. Cox, Alfred H. Merrill, Jr., Anthony H. Futerman

Correspondence

tony.futerman@weizmann.ac.il

In Brief

The variable phenotypes of Gaucher disease (GD) and other lysosomal storage disorders may be due to environmental and genetic factors. Here, Klein et al. induce Gaucher disease in 15 inbred mouse strains. Using a genome-wide association study, they identify 17 putative modifier genes, among them NR2B, the B subunit of the NMDA receptor.

Highlights

- Gaucher disease displays considerable phenotypic variability

- Genetic variation of mouse strains is used to map Gaucher disease modifier genes

- A combination of genotypes predicts the severity of Gaucher disease

- An antagonist of the NMDA receptor increases the lifespan of GD mice

Accession Numbers

GSE78757

CrossMark

CellPress

Identification of Modifier Genes
in a Mouse Model of Gaucher Disease

Andrés D. Klein,[1,6] Natalia-Santos Ferreira,[1] Shifra Ben-Dor,[2] Jingjing Duan,[3] John Hardy,[4] Timothy M. Cox,[5] Alfred H. Merrill, Jr.,[3] and Anthony H. Futerman[1,7,*]
[1]Department of Biomolecular Sciences
[2]Department of Biological Services
Weizmann Institute of Science, Rehovot 76100, Israel
[3]School of Biology and Petit Institute for Bioengineering and Bioscience, Georgia Institute of Technology, Atlanta, GA 30318, USA
[4]University College London, Institute of Neurology, London WC1N 3BG, UK
[5]Department of Medicine, University of Cambridge, Cambridge CB2 1TN, UK
[6]Present address: Telethon Institute of Genetics and Medicine, Pozzuoli 80078, Italy
[7]Lead Contact
*Correspondence: tony.futerman@weizmann.ac.il
 http://dx.doi.org/10.1016/j.celrep.2016.07.085

SUMMARY

Diseases caused by single-gene mutations can display substantial phenotypic variability, which may be due to genetic, environmental, or epigenetic modifiers. Here, we induce Gaucher disease (GD), a rare inherited metabolic disorder, by injecting 15 inbred mouse strains with a low dose of a chemical inhibitor of acid β-glucosidase, the enzyme defective in GD. Different mouse strains exhibit widely different lifespans, which is unrelated to levels of acid β-glucosidase's substrate accumulation. Genome-wide association reveals a number of candidate risk loci, including a marker within Grin2b, which in combination with another marker allows us to predict the lifespan of additional mouse strains. An antagonist of the NMDA receptor (encoded by Grin2b) significantly increases the lifespan of GD mice that would otherwise have lived for a short time. Our data identify putative modifier genes that may be involved in determining GD severity, which might help elucidate phenotypic variability between patients with similar GD mutations.

INTRODUCTION

Monogenic diseases frequently present with a wide spectrum of disease symptoms such that genotype-phenotype correlations are often poor and identical mutations may trigger diverse phenotypes (Argmann et al., 2016). A classic example is Gaucher disease (GD), a rare lysosomal storage disorder (LSD) caused by mutations in the *GBA1* gene, in which some patients display systemic disease with little or no neurological involvement while others display an aggressive neurological disease (nGD) (Grabowski et al., 2013). Moreover, heterozygous and homozygous mutations in *GBA1* are the highest known genetic risk factor

for the development of Parkinson's disease (PD) and dementia with Lewy bodies (DLB) (Schiffmann and Vellodi, 2007; Nalls et al., 2013). Thus, it is becoming clear that the one gene/one disease paradigm needs re-evaluating (Gropman and Adams, 2007).

The typical way to study genetic modifiers of disease are linkage and association studies, although large multi-scale omic technologies and network approaches might provide an alternative approach (Argmann et al., 2016). In this study, we took advantage of the availability of conduritol β-epoxide (CBE), an inhibitor of acid β-glucosidase (GCase), the enzyme defective in GD. CBE has been widely used to induce GD in mice (Farfel-Becker et al., 2011a; Vardi et al., 2016), but most studies use high amounts of CBE, which can lead to rapid death and therefore mask phenotypic variability. We used a lower dose of CBE and injected 15 inbred mouse strains from diverse phylogenetic origins whose SNP profiles are available. A genome-wide association study (GWAS) identified putative modifier genes, allowed prediction of phenotypic variability in additional mouse strains, and suggested a possible therapeutic target for nGD. We suggest that this approach could be used for studying phenotypic variability in other inborn errors of metabolism.

RESULTS

Phenotypic Variability of Inbred Mouse Strains upon CBE Injection

Genetic background influences the severity of LSDs in mice, although typically such studies are performed using only two or three mouse strains (Kovács and Pearce, 2015; Parra et al., 2011). We tested phenotypic variability in 15 inbred mouse strains that have each undergone >20 generations of inbreeding, are from diverse phylogenetic origins (Figure 1A), and for whom SNP profiles (Kirby et al., 2010) are available (http://phenome.jax.org). Male mice were injected daily with 25 mg CBE/kg body weight starting at post-natal day 8. A substantial difference in lifespan was observed (Figure 1B), with some strains dying by 50 days of age (A/J, AKR/J, C3H/HeJ, DBA/2J,
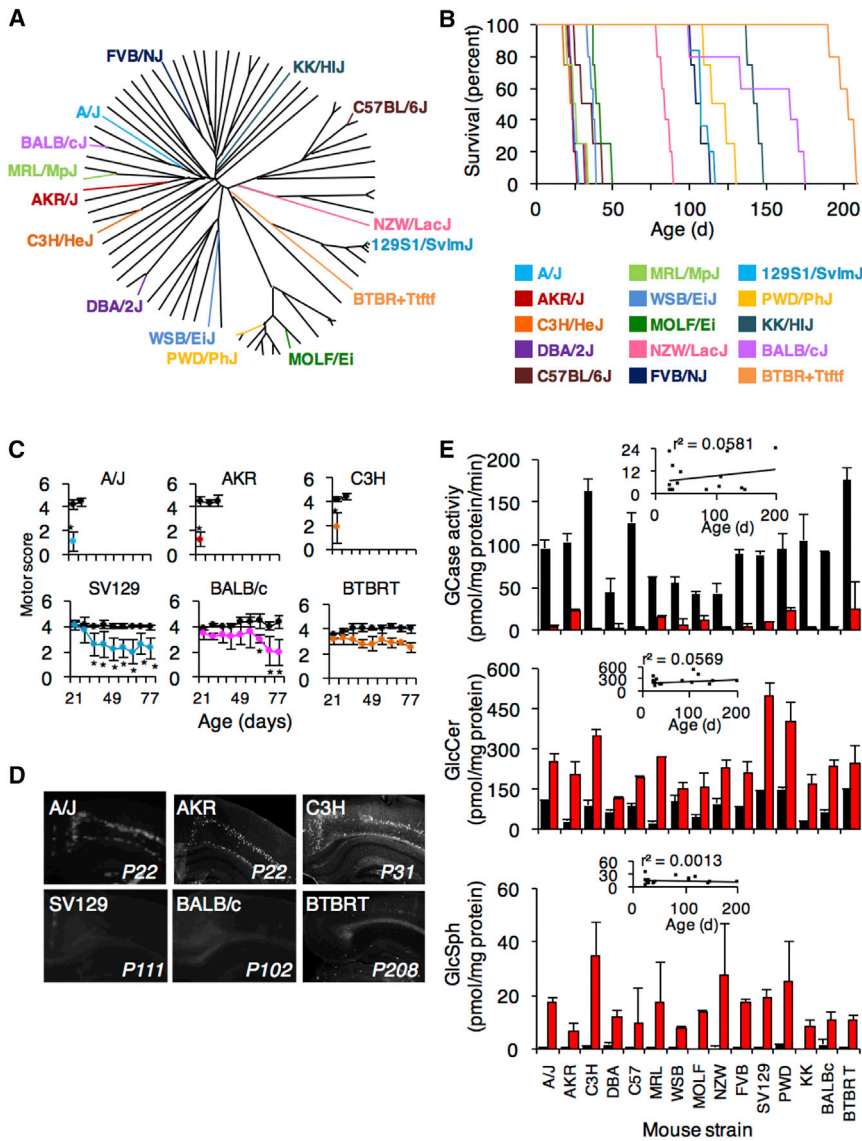
Figure 1. Variation in Lifespan among Mouse Strains upon CBE Injection

(A) Phylogenetic tree of 94 inbred mouse strains (adapted from Kirby et al., 2010, with permission from the Genetics Society of America). The 15 mouse strains used in this study are highlighted in color.

(B) Each mouse strain was injected daily i.p. with 25 mg CBE/kg body weight from post-natal day (P)8. Mouse survival is shown as a Kaplan-Meier survival plot and is color-coded as in (A) (n = 4–9 per mouse strain). Note that there was no correlation between lifespan and the initial weight of the mice on P8 ($r^2 = 0.074$) nor between the lifespan of untreated mouse strains (Yuan et al., 2009) and lifespan upon CBE treatment ($r^2 = 0.007$).

(C) Motor coordination was determined by the hanging wire test. Mice injected with PBS, black circles; mice injected with CBE, colored circles (color coded as in A). Results are means ± SEM (n = 4–5 per strain, *p < 0.05).

(D) CD68 immunofluorescence in layer V of the cortex. The age (days) at which the analysis was performed is shown in italics.

(E) GCase activity and GlcCer and GlcSph levels in mice injected daily with PBS (black bars) or with CBE (red bars) from P8–18. Values are means ± SEM (n = 2 for analyses performed in duplicate). The inset shows the lack of correlation (r^2) between the lifespan of the mice and the extent of CBE inhibition or levels of GlcCer and GlcSph accumulation upon CBE injection.

C57BL/6JOlaHsd, MRL/MpJ, WSB/EiJ, and MOLF/Ei; short-lived strains) while others lived for 80–200 days (NZW/LacJ, FVB/NJ, 129S1/SvImJ, PWD/PhJ, BALB/cJ, KK/HiJ, and BTBR T+ Itpr³ᵗᶠ/J; long-lived strains). Strains with a short lifespan had pronounced motor defects (Figures 1C and S1), whereas those with a longer lifespan developed motor abnormalities at a later age (Figure 1C). Moreover, mice that lived for a short time displayed activated microglia in layer V of the cortex, an area that shows significant pathology in mouse models of nGD (Farfel-Becker et al., 2011b; Vitner et al., 2014). Few, if any, activated microglia were detected in the same region in long-lived strains, even at later stages of the disease (Figure 1D), suggesting that mice with a long lifespan may die from non-neurological disease.

Although basal GCase activity varied somewhat among different strains, the extent of GCase inhibition in the brain by CBE was 90%–95% in all strains, and there was no correlation

between lifespan and basal GCase activity ($r^2 = 0.13$) or the extent of inhibition by CBE ($r^2 = 0.06$) (Figure 1E). We also determined levels of the two sphingolipid substrates that accumulate in GD, glucosylceramide (GlcCer) and glucosylsphingosine (GlcSph). Differences in lipid levels were apparent between strains, but no correlation was found between lifespan and basal GlcCer ($r^2 = 0.14$) or GlcSph ($r^2 = 0.07$) level or with increased GlcCer/GlcSph levels upon CBE treatment (Figure 1E); furthermore, there was no correlation between levels of two other sphingolipids, galactosylceramide ($r^2 = 0.01$) and galactosylsphingosine ($r^2 = 0.01$), and lifespan (Figure S2). These results demonstrate that lipid accumulation is necessary, but not sufficient, to trigger neurological disease in nGD, and they exclude the possibility of differential metabolism of CBE in different mouse strains. Moreover, there is no correlation between the life expectancies of untreated mouse strains (http://phenome.jax.org) (Yuan et al., 2009) and lifespan after CBE injection. This demonstrates an unexpected level of phenotypic variability between mouse strains upon CBE injection, implying a role for genetic modifiers as determinants of GD severity.

Identification of Putative Genetic Modifiers

We performed a GWAS using the efficient mixed-model association (EMMA) algorithm, which corrects for population structure
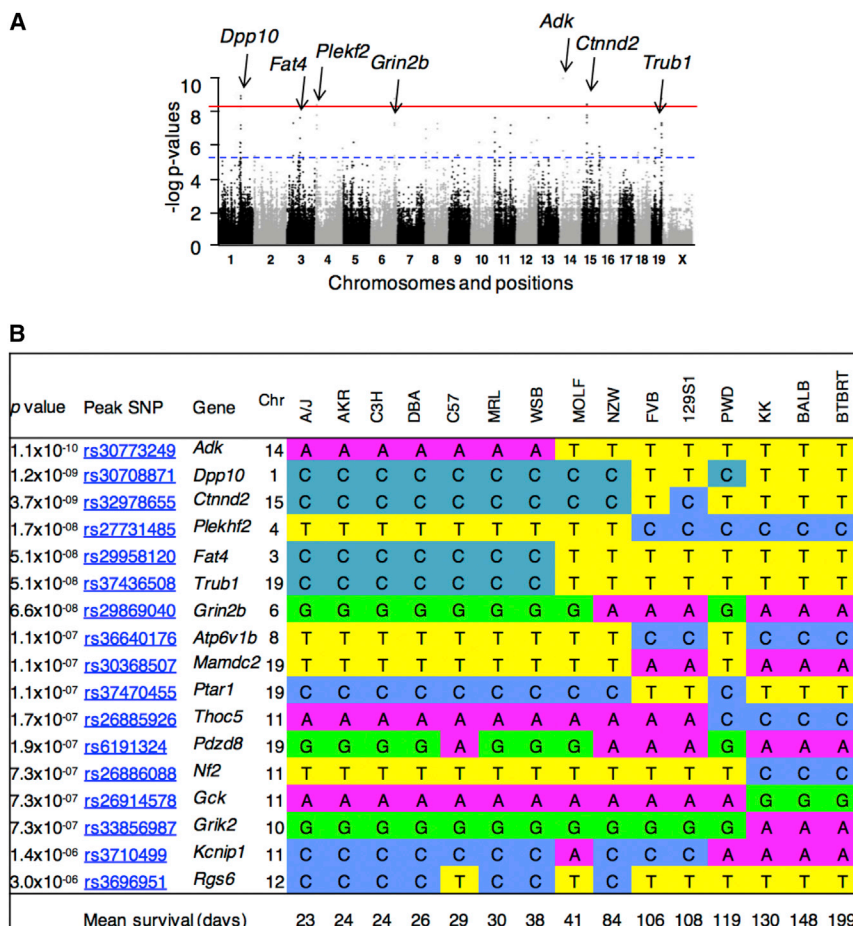
Figure 2. Identification of Putative Modifier Genes by GWAS

(A) Manhattan plot showing the −log10 of the odds of association of the markers in each chromosome. The threshold of significance is indicated (red line) as are the suggestive threshold (blue line) and the top associated genes.

(B) Strains organized according to average lifespan and the genotypes of the peak-associated SNPs per gene. Note that the PWD/PhJ strain appears to be an outlier since it displayed a different pattern of distribution of the genotypes among the long-lived strains, perhaps due to its wild-derived origin (Kirby et al., 2010). Adenine (A), magenta; cytosine (C), blue; guanine (G), green; thymine (T), yellow; Chr, chromosome. Further details about the functions of these genes and the diseases with which they are associated are given in Table S2.

p value	Peak SNP	Gene	Chr	A/J	AKR	C3H	DBA	C57	MRL	WSB	MOLF	NZW	FVB	129S1	PWD	KK	BALB	BTBRT
1.1x10⁻¹⁰	rs30773249	Adk	14	A	A	A	A	A	A	A	T	T	T	T	T	T	T	T
1.2x10⁻⁰⁹	rs30708871	Dpp10	1	C	C	C	C	C	C	C	C	C	T	T	C	T	T	T
3.7x10⁻⁰⁹	rs32978655	Ctnnd2	15	C	C	C	C	C	C	C	C	C	T	C	T	T	T	T
1.7x10⁻⁰⁸	rs27731485	Plekhf2	4	T	T	T	T	T	T	T	T	T	C	C	C	C	C	C
5.1x10⁻⁰⁸	rs29958120	Fat4	3	C	C	C	C	C	C	C	T	T	T	T	T	T	T	T
5.1x10⁻⁰⁸	rs37436508	Trub1	19	C	C	C	C	C	C	C	T	T	T	T	T	T	T	T
6.6x10⁻⁰⁸	rs29869040	Grin2b	6	G	G	G	G	G	G	G	A	A	A	G	A	A	A	A
1.1x10⁻⁰⁷	rs36640176	Atp6v1b	8	T	T	T	T	T	T	T	T	T	C	C	T	C	C	C
1.1x10⁻⁰⁷	rs30368507	Mamdc2	19	T	T	T	T	T	T	T	T	T	A	A	T	A	A	A
1.1x10⁻⁰⁷	rs37470455	Ptar1	19	C	C	C	C	C	C	C	C	C	T	T	C	T	T	T
1.7x10⁻⁰⁷	rs26885926	Thoc5	11	A	A	A	A	A	A	A	A	A	A	C	C	C	C	C
1.9x10⁻⁰⁷	rs6191324	Pdzd8	19	G	G	G	G	A	G	G	G	A	A	A	G	A	A	A
7.3x10⁻⁰⁷	rs26886088	Nf2	11	T	T	T	T	T	T	T	T	T	T	T	C	C	C	C
7.3x10⁻⁰⁷	rs26914578	Gck	11	A	A	A	A	A	A	A	A	A	A	A	A	G	G	G
7.3x10⁻⁰⁷	rs33856987	Grik2	10	G	G	G	G	G	G	G	G	G	G	G	G	A	A	A
1.4x10⁻⁰⁶	rs3710499	Kcnip1	11	C	C	C	C	C	C	C	A	C	C	C	A	A	A	A
3.0x10⁻⁰⁶	rs3696951	Rgs6	12	C	C	C	C	T	C	C	T	C	T	T	T	T	T	T
Mean survival (days)				23	24	24	26	29	30	38	41	84	106	108	119	130	148	199

and cofounding effects (Kang et al., 2008), based on the lifespans of the mouse strains upon CBE injection. The genome-wide Bonferroni threshold of significance was 1.25×10^{-8}, and suggestive associations were considered from $p = 4.1 \times 10^{-6}$ (Kang et al., 2008) (Figure 2A). We analyzed SNPs residing within genes and identified 17 genes. All of the identified SNPs were located in introns (with the exception of rs27731485, which was located at the 3′ UTR region of *Plekhf2*). Mouse strains were organized by lifespan and a matrix was plotted using the genotypes of the SNPs (Figure 2B). Short-lived strains showed a pattern of distribution of genotypes that differed from long-lived strains, and strains with intermediate lifespans displayed intermediate patterns.

To test whether a combination of markers could predict the severity of nGD, we analyzed the SNP profiles of other mouse strains. No additional strains shared the distribution of genotypes as the short-lived strains (i.e., A/J, AKR/J, and C3H/HeJ) or the long-lived strains (i.e., BALB/cJ, KK/HiJ, and BTBR T⁺ Itpr3ᵗᶠ/ᴶ). We consequently analyzed the genomic regions where the SNPs reside, by downloading the genomic data (http://www.sanger.ac.uk/science/data/mouse-genomes-project) available for the strains used in our study, to determine the best candidates for predicting lifespan. We chose rs32982614, which resides within *Ctnnd2*, and rs29869040, which resides in *Grin2b*, as they

delineate between short- and long-lived strains. BPL/1J and I/LnJ mouse strains shared the genotypes of the short-lived strains (Figure 3A), and P/J and BPN/3J shared the genotypes of the long-lived strains for these SNPs (Figure 3A). We injected these mice (Figure 3B) with CBE, and our predictions with respect to lifespan were validated (Figure 3C). Finally, we performed an additional GWAS using mouse strains that lived for >80 days, since they displayed significant variation in lifespan. Additional SNPs were found in *Mgat5*, *Aff2*, and *Tox3*, and in two uncharacterized genes (Figure S3; Table S3).

To discover genes involved in the susceptibility or resistance to develop neurological disease, we performed microarray analysis in cortex, one of the most significantly affected brain areas in nGD (Farfel-Becker et al., 2011b), in short-lived (C57BL/6JOlaHsd and C3H/HeJ) and long-lived (FVB/NJ and 129S1/SvImJ) strains in PBS- and CBE-treated mice (n = 3 per condition). On day 18, 161 genes displayed differential expression between short- and long-lived strains (>1.5-fold change, corrected $p < 0.05$) upon PBS injection, while 228 genes differed in mice injected with CBE (Table S3). Importantly, of these, 116 were common (Figure 3D) irrespective of whether they were treated with PBS or CBE. Most of the 116 genes have unknown functions, but 24 are genes for non-coding RNAs, including long non-coding RNAs, pseudogenes, and microRNAs. Domain analysis (Figure 3E) revealed that the takusan family was highly enriched in these 116 genes ($p = 1.3^{-37}$), and members were expressed at lower levels in the short- versus long-lived strains (Figure 3F), a finding validated by qPCR using primers flanking the *2610042L04Rik* gene in two short-lived (A/J and C57BL/6JOlaHsd) and two long-lived (FVB/NJ and NZW/LacJ) strains (Figure 3G). The takusan family is involved in the interaction of postsynaptic molecules with both NMDA and AMPA glutamate receptors (Tu et al., 2007), suggesting a fundamental difference in synaptic function between short- and long-lived strains.
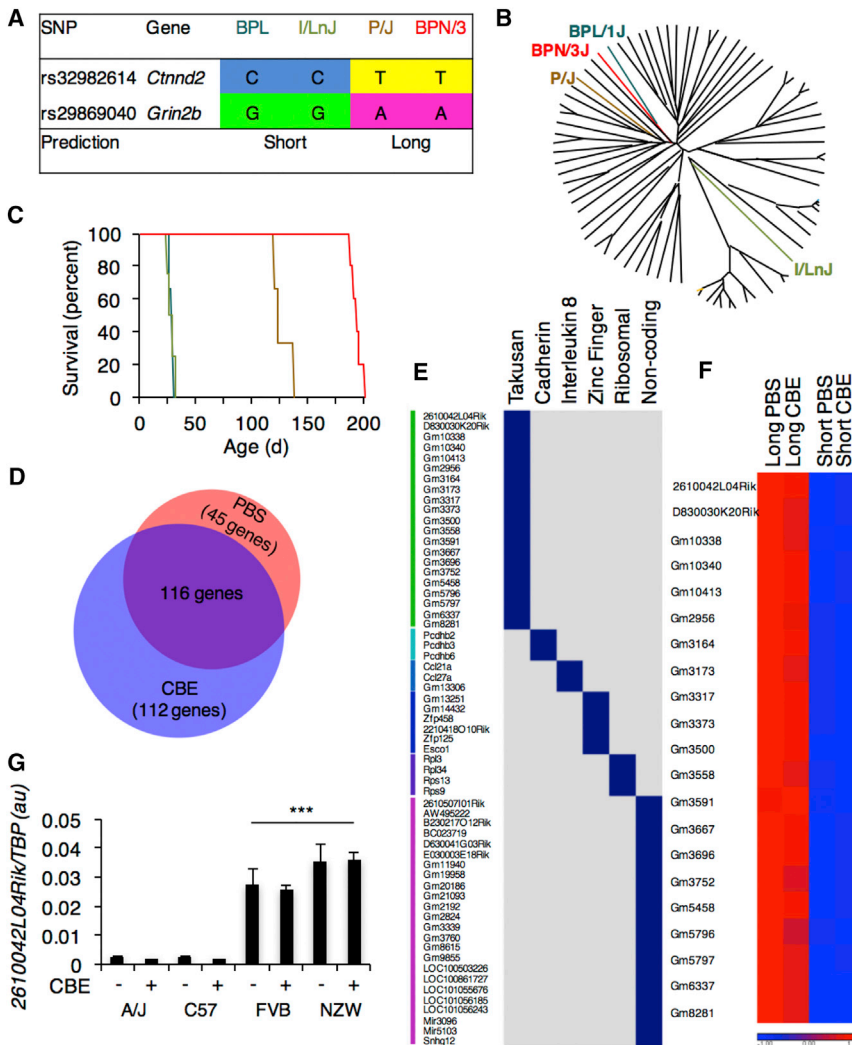
Figure 3. Predictive Value of a Combination of SNPs

(A) Genotypes of the predicted short- and long-lived mouse strains are shown.

(B) Phylogenetic tree highlights the four additional strains used to predict lifespan.

(C) Kaplan-Meier survival curves of strains injected daily with CBE starting at P8. Mouse strains are color coded as in (A) (n = 3–5).

(D) Venn diagram shows differentially regulated genes between short- and long-lived strains.

(E) Classification of differentially regulated genes in short- versus long-lived strains. PFAM domains (Finn et al., 2016), which are found in at in least three proteins, as well as the non-coding genes are shown. Details can be found in Table S4.

(F) Heatmap shows differential expression of the takusan family genes.

(G) qPCR of 2610042L04Rik in cortical homogenates from 18-day-old PBS- and CBE-treated A/J, C57BL6/JOlaHsd (C57), FVB/NJ (FVB), and NZW/LacJ (NZW) mice. Results are means ± SEM (n = 3 per condition, ***p < 0.001 between short- and long-lived strains).

gression of motor symptoms (Figure 4E), and a delay in appearance of activated microglia (Figure 4F). Moreover, two proteins recently implicated in nGD pathogenesis, the cleaved form of receptor-interacting protein kinase 1 (RipK1) (Vitner et al., 2014) and double-stranded RNA (dsRNA)-activated protein kinase (PKR) (Vitner et al., 2016), were significantly reduced (Figure 4G), suggesting that activation of the RipK pathway in GD may occur downstream of NR2B. The unlikely possibility that memantine affects the efficacy of GCase inhibition by CBE was excluded by demonstrating that GCase was inhibited to a similar extent with or without memantine (Figure 4H). The lifespan of Gba$^{flox/flox}$;nestin-Cre mice, which display severe neurological symptoms and die at 3 weeks of age (Farfel-Becker et al., 2011b), also was extended to a small but significant extent (p < 0.001) using a higher dose of memantine (Figure 4I).

Finally, we examined levels of NR2B in post-mortem human brain tissue obtained from type 1 (systemic disease, no neurological symptoms), type 2 (severe, acute neurological disease, infantile death), and type 3 GD (chronic neurological disease, juvenile death) (Pelled et al., 2005). NR2B levels were highest in the two available type 2 GD human brains (Figure 4J). We suggest that Grin2b modulation might be able to modify the severity of GD pathology and is a potential therapeutic target.

Role of NR2B in nGD

A number of the genes identified by GWAS are involved in the regulation of glutamate-related pathways in the brain, including Adk, Ctnnd2, Grik2, and Grin2b (Table S2), consistent with earlier studies suggesting a role for glutamate in nGD pathology (Korkotian et al., 1999; Pelled et al., 2005). Grin2b encodes for NR2B, the B subunit of the NMDA glutamate receptor. Analysis of Grin2b mRNA levels in cortex demonstrated upregulation in the short-lived strains (p < 0.05) (Figure 4A). Treatment of A/J, C57BL/6JOlaHsd, C3H/HeJ, and DBA/2J strains with memantine, an FDA-approved NMDA antagonist for use in moderate-to-severe Alzheimer's disease (Aarsland et al., 2009; Howard et al., 2012), and CBE significantly increased their lifespan compared to mice treated with CBE alone (Figure 4B), whereas activation of the NMDA receptor by D-cycloserine (D-Ser) (Danysz and Parsons, 1998) decreased the lifespan of BALB/cJ mice (Figure 4C) and that of three other long-lived strains (129S1/SvlmJ, FVB/NJ, and BTBR T$^+$ Itpr$^{3tf/J}$; data not shown).
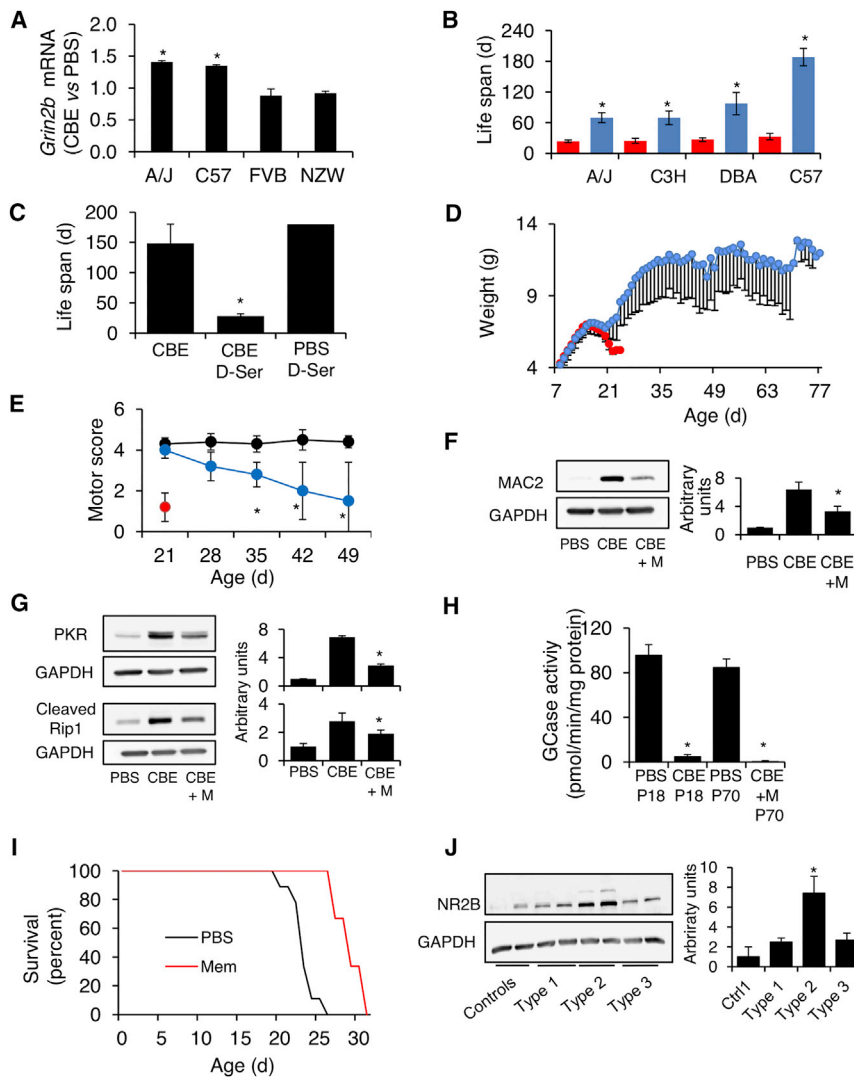
Upon memantine treatment, we observed a reduction in the rate of weight loss (Figure 4D), a delay in appearance and pro-

DISCUSSION

The genetic diversity of inbred mouse strains previously has been exploited to uncover genes involved in metabolic and toxicological traits and in viral infections and others (Crowley et al.,

Figure 4. Antagonism of NR2B Improves Neurological Symptoms in GD Mice

(A) qPCR of *Grin2b* in cortical homogenates from 18-day-old PBS- and CBE-treated A/J, C57BL6/JOlaHsd (C57), FVB/NJ (FVB), and NZW/LacJ (NZW) mice. Results are shown as fold change of the means ± SEM (n = 3 per condition, *p < 0.05).

(B) Average survival times of mouse strains injected daily with CBE (red bars) or CBE + memantine (3 mg/kg) (blue bars) starting on P8. Values are means ± SD (A/J, n = 10; DBA, n = 5–10; C3H/HeJ (C3H), n = 3–7; C57BL6/JOlaHsd (C57), n = 3–9; *p < 0.05).

(C) Average survival times of BALB/cJ mice injected daily with CBE ± D-Ser or PBS + D-Ser. The PBS + D-Ser mice were sacrificed at P180. Values are means ± SD (CBE, n = 5; CBE + D-Ser, n = 6; PBS + D-Ser, n = 3; *p < 0.05 compared to CBE).

(D) Body weight of A/J mice injected daily with CBE (red) ± memantine (blue) is shown (n = 10).

(E) Motor coordination determined by the hanging wire test in AJ mice treated with PBS (black), CBE (red), or CBE ± memantine (blue) as in (A). Values are means ± SEM (n = 4–5, *p < 0.05).

(F) Western blot of Mac2 in homogenates (75 μg protein) from brains of C57BL6/JOlaHsd mice treated as indicated at P30. Quantification is means ± SD (n = 3). M, memantine.

(G) PKR and Rip1 levels in homogenates (75 μg protein) from the brains of C57 mice treated as indicated at P30 are shown.

(H) GCase activity measured on the indicated days (P) of A/J mice injected daily with PBS, CBE, or CBE + memantine (3 mg/kg). Values are means ± SD (n = 2 in duplicate, *p < 0.001).

(I) Kaplan-Meier survival curves of Gba^flox/flox; nestin-Cre mice injected daily with PBS (n = 9) or 30 mg/kg body weight memantine (n = 6, p < 0.001) are shown.

(J) Western blots of NR2B in samples (90 μg protein) of human GD brain, with quantification. The genotypes of the samples from left to right are as follows: type 1, N370S/c.208delC and N370S/N370S; type 2, IVS2 + 1GNA/F251L and IVS2 + 1GNA/L444P; and type 3, D409H/L444P + Dup and G377S/g.5245delT (Pelled et al., 2005) (*p < 0.05).

2012; Parks et al., 2013; Rasmussen et al., 2014). However, the current study uses this approach to uncover modifier genes in a mouse model of a monogenic disease, and, in principle, this could be used for other inbred errors of metabolism, provided that suitable methods are available to induce disease. In this respect, GD is prototypical since it can be easily and rapidly induced by CBE in a time- and dose-dependent manner (Vardi et al., 2016).

Ours is not the first attempt to discover modifier genes for GD. For instance, *SCARB2* was suggested as a risk factor for developing an epileptic phenotype in type 3 GD (Velayati et al., 2011), and other studies have implicated glucosylceramide synthase, GBA2, GBA3, vitamin D receptor, IL-6, and TNF-α as possible modifiers, but no consistent correlation was observed with disease severity (Beutler and West, 2002; Altarescu et al., 2003, 2005; Dekker et al., 2011; Greenwood et al., 2010). GWAS also was per-

formed in a cohort of Jewish patients homozygous for the N370S mutation, and the results suggested CLN8 as a candidate modifier gene for type 1 GD, although genome-wide significance was not met after Bonferroni corrections (Zhang et al., 2012).

No significant associations in loci encoding for genes related to sphingolipid metabolism or in genes associated with aging and/or longevity (i.e., *Apoe1*, *Foxo3A*, and *Igf1*) (Peters et al., 2015) were detected. Genes with the highest significance in our GWAS, i.e., *Adk*, *Dpp10*, *Ctnnd2*, and *Grin2b*, are all involved in pathways related to neuronal excitability. Others such as *Plekhf2* and *Atp6v1b2* play critical roles in endolysosomal biology, and *Fat4* and *Nf2* are critical for brain development, suggesting that aspects of electrophysiology, neurodevelopment, and endolysosomal function may determine whether mice develop nGD, a notion supported by the potential role of the takusan family.

Additional information can be derived from our study on the role of specific genes in nGD pathogenesis. First, the C57BL/6JOlaHsd strain that we used does not express α-synuclein (Specht and Schoepfer, 2001), and the C3H/HeJ strain has an inactivating mutation in Toll-like receptor 4 (Poltorak et al., 1998); since both of these mice had a short lifespan, we can conclude that these proteins may be dispensable for development of the most aggressive forms of nGD. Second, evaluation of autistic-like behavior (Moy et al., 2007) in nine of the same inbred mouse strains used in our study demonstrated that most mouse strains that have short lifespans showed higher social behaviors, while most long-lived strains presented with autistic-like behavior. Autism spectrum disorders are hypoglutamatergic disorders (Vahabzadeh et al., 2015) that can be caused by loss of function in *GRIN2B* (Pan et al., 2015), consistent with the notion that alterations in NR2B might contribute to the susceptibility and resistance to developing autism and possibly to the development of mild versus aggressive forms of GD.

One of the most noteworthy findings from our study is the possible use of memantine as a therapy for nGD. Whether memantine could be used as a therapeutic option in human nGD patients remains to be established, as does the possibility that SNPs or mutations in the same genes discovered in our mouse GWAS might be predictive for the development of neurological symptoms in human GD patients. Although some mutations in the human *GBA1* gene predispose toward neurological disease (i.e., L444P) (Grabowski et al., 2013), it is essentially impossible to predict the course of disease development for most GD patients, particularly for compound heterozygotes. Whether the genes identified in our study might lead to such predictions and whether any of the genes might lead to unraveling the elusive connection between GD and PD and LSD remain to be established.

EXPERIMENTAL PROCEDURES

GD Mouse Models
Pure inbred mouse strains (BTBR T[+] Itpr3[tf/J], C3H/HeJ, DBA/2J, MRL/MpJ, WSB/EiJ, MOLF/Ei, PWD/PhJ, KK/HiJ, BPL/1J, I/LnJ, BPN/3J, and LP/J) were from Jackson Laboratory, Harlan UK (A/J, AKR/J, NZW/LacJ, and 129S1/SvImJ), and Harlan (C57BL/6JOlaHsd, BALB/cJ, and FVB/NJ). Male mice were injected daily intraperitoneally (i.p.) with 25 mg/kg body weight CBE (Calbiochem Millipore) with or without memantine (Sigma-Aldrich) (3 mg/kg body weight/day) or with D-Ser (Sigma-Aldrich) (200 mg/kg/day), starting from post-natal day 8 (Vitner et al., 2014). Motor coordination was evaluated weekly by the hanging wire test (Alvarez et al., 2008) as documented in the Supplemental Experimental Procedures. Gba[flox/flox];nestin-Cre mice (Enquist et al., 2007; Farfel-Becker et al., 2011b) were injected daily i.p. with 30 mg memantine/kg body weight from P8. Mice were maintained under specific pathogen-free conditions in the Experimental Animal Center of the Weizmann Institute of Science, and they were handled according to protocols approved by the Weizmann Institute Animal Care Committee according to international guidelines.

Immunofluorescence
Free-floating coronal brain sections (40 μm) were blocked for 1 hr with 2% BSA/0.2% Triton X-100 in PBS and incubated overnight with a rat anti-CD68 antibody (1:1,000; Serotec). CD68 was detected using a Cy3-conjugated donkey anti-rat antibody (1:200; Jackson ImmunoResearch Laboratories).

GCase Activity Assay and Sphingolipid Analysis
GCase activity and sphingolipid analysis were measured as described (Farfel-Becker et al., 2014). Additional details can be found in the Supplemental Experimental Procedures.

GWAS
GWA mapping was performed, using the lifespan of the inbred mouse strains injected with CBE, by EMMA using individual SNP associations (Kang et al., 2008). EMMA corrects for genetic relatedness and population structure, minimizing false associations. To assure high-resolution mapping of the mouse genome, the association was performed using 4,000,000 SNPs per strain. The SNP profiles of each strain were downloaded from http://mouse.cs.ucla.edu/mousehapmap/full.html. Each SNP was evaluated individually and p values were recorded as the strength of the genotype-phenotype associations. The threshold for genome-wide significance after stringent Bonferroni correction was 1.25×10^{-8} (Bland and Altman, 1995). Although a p value of 4.1×10^{-6} previously has been considered significant for GWA using EMMA in the hybrid mouse diversity panel (HMDP) (Kang et al., 2008), we considered this threshold as a suggestive value for associations. The Manhattan plot was generated using the R package (Turner, 2014).

Gene Array Analysis
See the Supplemental Experimental Procedures.

Western Blotting
Western blotting on mouse and human samples was performed as described in Vitner et al. (2014) and in the Supplemental Experimental Procedures.

Real-Time PCR
Real-Time PCR was performed as described (Vitner et al., 2014). Primer sets and conditions are described in the Supplemental Experimental Procedures.

Statistical Analysis
Comparison between two samples was performed using a two-tailed Student's t test and between multiple groups using one- and two-way ANOVA followed by the post hoc Turkey's test. Data were considered statistically significant when $p < 0.05$.

ACCESSION NUMBERS

The accession number for the microarray data reported in this paper is GEO: GSE78757.

SUPPLEMENTAL INFORMATION

Supplemental Information includes Supplemental Experimental Procedures, three figures, and four tables and can be found with this article online at http://dx.doi.org/10.1016/j.celrep.2016.07.085.

AUTHOR CONTRIBUTIONS

A.D.K. designed and performed most of the experiments and helped write the manuscript. N.-S.F. performed additional crucial experiments and J.D. also helped with some experiments. S.B.-D., T.M.C., J.H., and A.H.M. helped with experimental design and planning. A.H.F. participated in experimental design, supervised, and funded the project, and wrote the manuscript.

ACKNOWLEDGMENTS

REFERENCES

Aarsland, D., Ballard, C., Walker, Z., Bostrom, F., Alves, G., Kossakowski, K., Leroi, I., Pozo-Rodriguez, F., Minthon, L., and Londos, E. (2009). Memantine in patients with Parkinson's disease dementia or dementia with Lewy bodies: a double-blind, placebo-controlled, multicentre trial. Lancet Neurol. 8, 613–618.

Altarescu, G., Phillips, M., Foldes, A.J., Elstein, D., Zimran, A., and Mates, M. (2003). The interleukin-6 promoter polymorphism in Gaucher disease: a new modifier gene? QJM 96, 575–578.

Altarescu, G., Zimran, A., Michelakakis, H., and Elstein, D. (2005). TNF-alpha levels and TNF-alpha gene polymorphism in type I Gaucher disease. Cytokine 31, 149–152.

Alvarez, A.R., Klein, A., Castro, J., Cancino, G.I., Amigo, J., Mosqueira, M., Vargas, L.M., Yévenes, L.F., Bronfman, F.C., and Zanlungo, S. (2008). Imatinib therapy blocks cerebellar apoptosis and improves neurological symptoms in a mouse model of Niemann-Pick type C disease. FASEB J. 22, 3617–3627.

Argmann, C.A., Houten, S.M., Zhu, J., and Schadt, E.E. (2016). A next generation multiscale view of inborn errors of metabolism. Cell Metab. 23, 13–26.

Beutler, E., and West, C. (2002). Polymorphisms in glucosylceramide (glucocerebroside) synthase and the Gaucher disease phenotype. Isr. Med. Assoc. J. 4, 986–988.

Bland, J.M., and Altman, D.G. (1995). Multiple significance tests: the Bonferroni method. BMJ 310, 170.

Crowley, J.J., Kim, Y., Szatkiewicz, J.P., Pratt, A.L., Quackenbush, C.R., Adkins, D.E., van den Oord, E., Bogue, M.A., Yang, H., Wang, W., et al. (2012). Genome-wide association mapping of loci for antipsychotic-induced extrapyramidal symptoms in mice. Mamm. Genome 23, 322–335.

Danysz, W., and Parsons, C.G. (1998). Glycine and N-methyl-D-aspartate receptors: physiological significance and possible therapeutic applications. Pharmacol. Rev. 50, 597–664.

Dekker, N., Voorn-Brouwer, T., Verhoek, M., Wennekes, T., Narayan, R.S., Speijer, D., Hollak, C.E.M., Overkleeft, H.S., Boot, R.G., and Aerts, J.M.F.G. (2011). The cytosolic β-glucosidase GBA3 does not influence type 1 Gaucher disease manifestation. Blood Cells Mol. Dis. 46, 19–26.

Enquist, I.B., Lo Bianco, C., Ooka, A., Nilsson, E., Månsson, J.-E., Ehinger, M., Richter, J., Brady, R.O., Kirik, D., and Karlsson, S. (2007). Murine models of acute neuronopathic Gaucher disease. Proc. Natl. Acad. Sci. USA 104, 17483–17488.

Farfel-Becker, T., Vitner, E.B., and Futerman, A.H. (2011a). Animal models for Gaucher disease research. Dis. Model. Mech. 4, 746–752.

Farfel-Becker, T., Vitner, E.B., Pressey, S.N.R., Eilam, R., Cooper, J.D., and Futerman, A.H. (2011b). Spatial and temporal correlation between neuron loss and neuroinflammation in a mouse model of neuronopathic Gaucher disease. Hum. Mol. Genet. 20, 1375–1386.

Farfel-Becker, T., Vitner, E.B., Kelly, S.L., Bame, J.R., Duan, J., Shinder, V., Merrill, A.H., Jr., Dobrenis, K., and Futerman, A.H. (2014). Neuronal accumulation of glucosylceramide in a mouse model of neuronopathic Gaucher disease leads to neurodegeneration. Hum. Mol. Genet. 23, 843–854.

Finn, R.D., Coggill, P., Eberhardt, R.Y., Eddy, S.R., Mistry, J., Mitchell, A.L., Potter, S.C., Punta, M., Qureshi, M., Sangrador-Vegas, A., et al. (2016). The Pfam protein families database: towards a more sustainable future. Nucleic Acids Res. 44 (D1), D279–D285.

Grabowski, G.A., Petsko, G.A., and Kolodny, E.H. (2013). Gaucher disease. In The Online Metabolic and Molecular Bases of Inherited Disease, D. Valle, A.L.

Beaudet, B. Vogelstein, K.W. Kinzler, S.E. Antonarakis, A. Ballabio, K.M. Gibson, and G. Mitchell, eds. (McGraw-Hill Medical).

Greenwood, A., Elstein, D., Zimran, A., and Altarescu, G. (2010). Effect of vitamin D receptor (VDR) genotypes on the risk for osteoporosis in type 1 Gaucher disease. Clin. Rheumatol. 29, 1037–1041.

Gropman, A.L., and Adams, D.R. (2007). Atypical patterns of inheritance. Semin. Pediatr. Neurol. 14, 34–45.

Howard, R., McShane, R., Lindesay, J., Ritchie, C., Baldwin, A., Barber, R., Burns, A., Dening, T., Findlay, D., Holmes, C., et al. (2012). Donepezil and memantine for moderate-to-severe Alzheimer's disease. N. Engl. J. Med. 366, 893–903.

Kang, H.M., Zaitlen, N.A., Wade, C.M., Kirby, A., Heckerman, D., Daly, M.J., and Eskin, E. (2008). Efficient control of population structure in model organism association mapping. Genetics 178, 1709–1723.

Kirby, A., Kang, H.M., Wade, C.M., Cotsapas, C., Kostem, E., Han, B., Furlotte, N., Kang, E.Y., Rivas, M., Bogue, M.A., et al. (2010). Fine mapping in 94 inbred mouse strains using a high-density haplotype resource. Genetics 185, 1081–1095.

Korkotian, E., Schwarz, A., Pelled, D., Schwarzmann, G., Segal, M., and Futerman, A.H. (1999). Elevation of intracellular glucosylceramide levels results in an increase in endoplasmic reticulum density and in functional calcium stores in cultured neurons. J. Biol. Chem. 274, 21673–21678.

Kovács, A.D., and Pearce, D.A. (2015). Finding the most appropriate mouse model of juvenile CLN3 (Batten) disease for therapeutic studies: the importance of genetic background and gender. Dis. Model. Mech. 8, 351–361.

Moy, S.S., Nadler, J.J., Young, N.B., Perez, A., Holloway, L.P., Barbaro, R.P., Barbaro, J.R., Wilson, L.M., Threadgill, D.W., Lauder, J.M., et al. (2007). Mouse behavioral tasks relevant to autism: phenotypes of 10 inbred strains. Behav. Brain Res. 176, 4–20.

Nalls, M.A., Duran, R., Lopez, G., Kurzawa-Akanbi, M., McKeith, I.G., Chinnery, P.F., Morris, C.M., Theuns, J., Crosiers, D., Cras, P., et al. (2013). A multicenter study of glucocerebrosidase mutations in dementia with Lewy bodies. JAMA Neurol. 70, 727–735.

Pan, Y., Chen, J., Guo, H., Ou, J., Peng, Y., Liu, Q., Shen, Y., Shi, L., Liu, Y., Xiong, Z., et al. (2015). Association of genetic variants of GRIN2B with autism. Sci. Rep. 5, 8296.

Parks, B.W., Nam, E., Org, E., Kostem, E., Norheim, F., Hui, S.T., Pan, C., Civelek, M., Rau, C.D., Bennett, B.J., et al. (2013). Genetic control of obesity and gut microbiota composition in response to high-fat, high-sucrose diet in mice. Cell Metab. 17, 141–152.

Parra, J., Klein, A.D., Castro, J., Morales, M.G., Mosqueira, M., Valencia, I., Cortés, V., Rigotti, A., and Zanlungo, S. (2011). Npc1 deficiency in the C57BL/6J genetic background enhances Niemann-Pick disease type C spleen pathology. Biochem. Biophys. Res. Commun. 413, 400–406.

Pelled, D., Trajkovic-Bodennec, S., Lloyd-Evans, E., Sidransky, E., Schiffmann, R., and Futerman, A.H. (2005). Enhanced calcium release in the acute neuronopathic form of Gaucher disease. Neurobiol. Dis. 18, 83–88.

Peters, M.J., Joehanes, R., Pilling, L.C., Schurmann, C., Conneely, K.N., Powell, J., Reinmaa, E., Sutphin, G.L., Zhernakova, A., Schramm, K., et al.; NABEC/UKBEC Consortium (2015). The transcriptional landscape of age in human peripheral blood. Nat. Commun. 6, 8570.

Poltorak, A., He, X., Smirnova, I., Liu, M.Y., Van Huffel, C., Du, X., Birdwell, D., Alejos, E., Silva, M., Galanos, C., et al. (1998). Defective LPS signaling in C3H/HeJ and C57BL/10ScCr mice: mutations in Tlr4 gene. Science 282, 2085–2088.

Rasmussen, A.L., Okumura, A., Ferris, M.T., Green, R., Feldmann, F., Kelly, S.M., Scott, D.P., Safronetz, D., Haddock, E., LaCasse, R., et al. (2014). Host genetic diversity enables Ebola hemorrhagic fever pathogenesis and resistance. Science 346, 987–991.

Schiffmann, R., and Vellodi, A. (2007). Neuronopathic Gaucher disease. In Gaucher Disease, A.H. Futerman and A. Zimran, eds. (Boca Raton, FL: Taylor and Francis Group), pp. 175–196.

Specht, C.G., and Schoepfer, R. (2001). Deletion of the alpha-synuclein locus in a subpopulation of C57BL/6J inbred mice. BMC Neurosci. *2*, 11.

Tu, S., Shin, Y., Zago, W.M., States, B.A., Eroshkin, A., Lipton, S.A., Tong, G.G., and Nakanishi, N. (2007). Takusan: a large gene family that regulates synaptic activity. Neuron *55*, 69–85.

Turner, S.D. (2014). qqman: an R package for visualizing GWAS results using Q-Q and manhattan plots. bioRxiv, 1–2. http://dx.doi.org/10.1101/005165.

Vahabzadeh, A., Landino, S.M., Finger, B.C., Carlezon, W.A., Jr., and McDougle, C.J. (2015). Neural targets in the study and treatment of social cognition in autism spectrum disorder. Handbook Exp. Pharmacol. *228*, 309–334.

Vardi, A., Zigdon, H., Meshcheriakova, A., Klein, A.D., Yaacobi, C., Eilam, R., Kenwood, B.M., Rahim, A.A., Massaro, G., Merrill, A.H., Jr., et al. (2016). Delineating pathological pathways in a chemically induced mouse model of Gaucher disease. J. Pathol. *239*, 496–509.

Velayati, A., DePaolo, J., Gupta, N., Choi, J.H., Moaven, N., Westbroek, W., Goker-Alpan, O., Goldin, E., Stubblefield, B.K., Kolodny, E., et al. (2011). A mutation in SCARB2 is a modifier in Gaucher disease. Hum. Mutat. *32*, 1232–1238.

Vitner, E.B., Salomon, R., Farfel-Becker, T., Meshcheriakova, A., Ali, M., Klein, A.D., Platt, F.M., Cox, T.M., and Futerman, A.H. (2014). RIPK3 as a potential therapeutic target for Gaucher's disease. Nat. Med. *20*, 204–208.

Vitner, E.B., Farfel-Becker, T., Ferreira, N.S., Leshkowitz, D., Sharma, P., Lang, K.S., and Futerman, A.H. (2016). Induction of the type I interferon response in neurological forms of Gaucher disease. J. Neuroinflammation *13*, 104.

Yuan, R., Tsaih, S.W., Petkova, S.B., Marin de Evsikova, C., Xing, S., Marion, M.A., Bogue, M.A., Mills, K.D., Peters, L.L., Bult, C.J., et al. (2009). Aging in inbred strains of mice: study design and interim report on median lifespans and circulating IGF1 levels. Aging Cell *8*, 277–287.

Zhang, C.K., Stein, P.B., Liu, J., Wang, Z., Yang, R., Cho, J.H., Gregersen, P.K., Aerts, J.M.F.G., Zhao, H., Pastores, G.M., and Mistry, P.K. (2012). Genome-wide association study of N370S homozygous Gaucher disease reveals the candidacy of CLN8 gene as a genetic modifier contributing to extreme phenotypic variation. Am. J. Hematol. *87*, 377–383.